

M. SZYMANEK\*, B. AUGUSTYN\*, D. KAPINOS\*, S. BOCZKAL\*, J. NOWAK\*\*

## PRODUCING ULTRAFINE GRAIN STRUCTURE IN AZ91 MAGNESIUM ALLOY CAST BY RAPID SOLIDIFICATION

### WYTWARZANIE MATERIAŁU O ULTRADROBNOZIARNISTEJ STRUKTURZE ZE STOPU MAGNEZU AZ91 ODLEWANEGO W PROCESIE RAPID SOLIDIFICATION

The paper presents the technological aspect of the process of casting, crushing and plastic consolidation of semi-finished products from magnesium alloy. The aim of this study was to produce by the rapid solidification process a magnesium alloy from the MgAl9Zn1 family in the form of ribbons with ultrafine grain structure. The material cast in the melt spinning device was next crushed and subjected to the operation of cold consolidation and hot extrusion. The paper presents different stages of the process, including initial characterisation of the obtained material.

*Keywords:* magnesium alloy, rapid solidification, plastic consolidation, hot extrusion, extrusion die profile

W artykule przedstawiono aspekt technologiczny procesu odlewania, rozdrabniania i konsolidacji plastycznej otrzymywanych półwyrobów ze stopu magnezu. Celem pracy było wytworzenie metodą szybkiej krystalizacji stopu magnezu z układu MgAl9Zn1, o ultradrobnoziarnistej strukturze w postaci taśmy. Materiał odlany na stanowisku melt spinning w kolejnym etapie został rozdrobniony i poddany procesowi konsolidacji na zimno i wyciskaniu na gorąco. W artykule zostały przedstawione poszczególne etapy procesu wraz z wstępną charakteryzacją otrzymywanego materiału.

#### 1. Introduction

Magnesium alloys are attractive materials for designers due to their good mechanical properties and low specific density. Materials with these characteristics are used in the automotive industry, in the land and air transport means. By reducing the kerb weight of vehicles, parts and components included, a real reduction in oil consumption, air emissions to the atmosphere, and operating costs is obtained. Another known method of reducing the weight of vehicles is by increasing the mechanical properties of structural materials and the effect of this increase is further translated into the reduced active sections and weight.

Known for many years, metal shaping operations by the processes of forging and extrusion of cast bars/ingots improve in most cases the mechanical, technological and functional properties.

The development of modern structures and metallic materials forces a continuous search for new methods of production and processing. The method of Rapid Solidification, due to the specific conditions of solidification comprised within the range of  $10^4$ - $10^6$  K/s, can produce materials with ultrafine grain structure from alloys with standard and customised chemical compositions. The melt spinning method has an additional advantage which consists in the possibility to produce mate-

rials with properties impossible to obtain in the conventional manufacturing processes.

When a thin stream of molten alloy is dropped onto a spinning copper wheel at an appropriate speed of 50 m/s, a strip (ribbon) is obtained. The ribbon cast by RS in EN-MC MgAl9Zn1- AZ91 alloy is characterised by a width comprised in the range of 1400-3000  $\mu\text{m}$  and a thickness of 50-100  $\mu\text{m}$ . This material is used as a feedstock in the following stages of processing such as: crushing, cold compacting and hot consolidation.

In the process of alloy production, and in the successive operations of the strip casting, crushing, consolidation and hot extrusion, it is possible to obtain shaped sections (Fig. 5) characterised by ultrafine grain structure and improved mechanical properties.

#### 2. Methodology

The authors of this study undertook the task of manufacturing a shaped profile from the EN-MCMgAl9Zn1 alloy by casting the metal in a melt spinning device according to the flow chart given below.

\* INSTITUTE OF NON FERROUS METALS, LIGHT METALS DIVISION IN SKAWINA, 19 PILSUDSKIEGO STREET, 32-050 SKAWINA, POLAND

\*\* PHD, FACULTY OF FOUNDRY ENGINEERING, AGH UNIVERSITY OF SCIENCE AND TECHNOLOGY IN CRACOW POLAND

Flow chart of the Rapid Solidification process

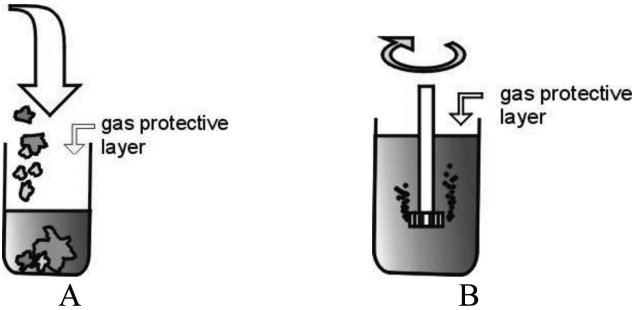


Fig. 1. STEP 1: Making RS alloy; A – melting and adding of alloying elements, B – gas refining of alloy melt + filtration

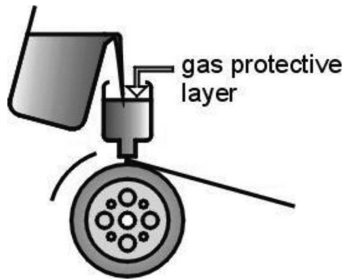


Fig. 2. STEP 2: Alloy casting by melt spinning



Fig. 3. STEP 3: Refining of cast ribbons

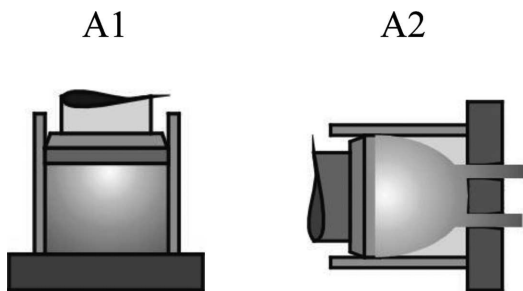


Fig. 4. STEP 4: Compacting, consolidation and extrusion of fine chips in the hot extrusion process and Continuous Rotary Extrusion; A1 – cold extrusion – degassing, A2 – Hot Extrusion

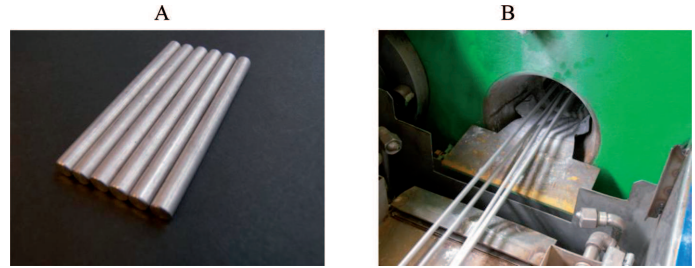


Fig. 5. A, B – Hot extrusion product

**Stage one** of the technological process began with searching for a magnesium alloy, which would be suitable for use in the transport means by air, sea or land, and which would be, moreover, covered by a standard. The team implementing the task chose the alloy with the following chemical composition, determining the average content of elements according to EN-MC MgAl9Zn1-AZ91 (the stated average numerical value of the elements is expressed as a weight-mass percentage). The charge for the alloy manufacture was based on primary magnesium (HP) with the addition of aluminium as a main alloying element and with Zn and Mn. Both aluminium and zinc were introduced in the form of lumps, while manganese was added as a master alloy. The alloy was melted in a resistance crucible furnace of special design; the maximum charge weight was 30 kg calculated in terms of Mg with the option of mechanical bath stirring. Additionally, the melt surface in the crucible was coated with protective mixture preventing the magnesium alloy oxidation. The manufacturing process of AZ91 alloy and casting of this alloy were performed in an air-tight system in a protective atmosphere of argon and a mixture of gases. The construction of the furnace allowed control of alloy temperature in the crucible and ingot casting chamber and control of the protective atmosphere in both crucible and ingot casting chamber. This arrangement allowed obtaining a high quality melt that was used for casting of ribbons by RS. The melt temperature during alloying was maintained in a range of 630 - 700°C to let all the alloying elements dissolve completely. Alloy purification was done by argon bubble refining technique and filtration. It should be noted that thus prepared EN-MC MgAl9Zn1-AZ91 alloy melt was not modified. Final chemical analysis of the alloy composition was made by mass spectrometry; the obtained values are shown in Table 1.

TABLE 1  
The result of final chemical analysis of the EN-MC MgAl9Zn1 alloy

| Element        | Mg   | Al   | Zn   | Mn   | Si    | Fe    |
|----------------|------|------|------|------|-------|-------|
| Content [ wt%] | 90.4 | 8.78 | 0.50 | 0.23 | 0.037 | 0.002 |

Then, the resulting alloy was cast into metal moulds in the form of 1.4 kg ingots and was used as a feedstock for further casting of ribbons in the melt spinning device.

**Second stage** of the technological process concerned RS casting of ribbons (Fig. 8) from the EN-MC MgAl9Zn1-AZ91 alloy using a 500 mm diameter copper wheel 70 mm wide, intensively cooled with a liquid. The melt spinning device used in this experiment was designed and constructed in earlier projects and adapted for casting of magnesium alloys. Feed-

ing of liquid alloy onto the surface of the rotating wheel was done from the top through a metering nozzle and gas cushion (Ar) ejecting the liquid alloy. The RS holding furnace used in the casting process stabilised the temperature of molten alloy. Melting of AZ91 ingots was carried out in a resistance furnace co-operating with the RS device. This method allowed rapid melting of the charge with mechanical stirring of the melt and gas protection. Additionally it reduced holding and segregation of alloying elements in a resistance furnace of the melt spinning device. The alloy casting temperature of 615 - 625°C (Fig. 6A, 6B and Table 2) was selected from the CC and FD curves. The curves obtained by the thermal analysis of EN-MC MgAl9Zn1-AZ91 alloy on an UMSA5/MTC\_MG apparatus (Universal Metallurgical Simulator and Analyzer) allowed accurate determination of the liquidus and solidus temperature of the batch of produced alloy. The overheating temperature of 13-23°C above the liquidus line protected the alloy against excessive oxidation and ensured a good fluidity.

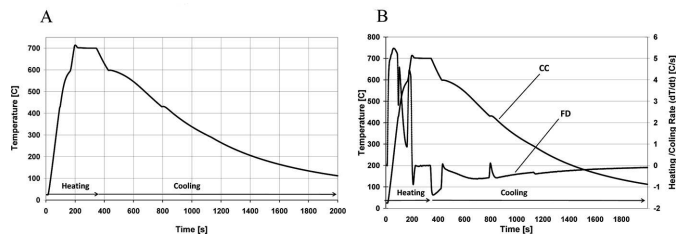


Fig. 6. A. Heating and cooling curve of the AZ91 alloy cast into metal mould; B. Superposing of the AZ91 alloy crystallisation curve (CC) and its first derivative (FD) in function of time (alloy cast into metal mould )

TABLE 2

Thermal characteristics of the AZ91 alloy test sample heating cycle

| No. | Thermal characteristics | Material poured into metal mould [°C] | Material from RS process [°C] |
|-----|-------------------------|---------------------------------------|-------------------------------|
| 1   | End of solidification   | 425                                   | 440                           |
| 2   | Start of solidification | 602                                   | 578                           |



Fig. 7. The appearance of RS ribbon cast from AZ91 alloy

The surface of the cast strip (Fig. 8A, 8B) was examined under a light microscope; the microstructure visible in the image was obtained at a magnification of 50x.

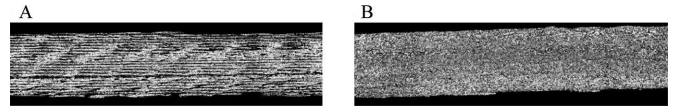


Fig. 8. A – Ribbon surface on the side contacting the atmosphere; B – Ribbon surface on the side contacting the Cu wheel

It is easy to note the difference in the morphology of the ribbon surface on the side contacting the atmosphere (Fig. 8A) and on the side contacting the moulding wheel (Fig. 8B). Comparing the AZ91RS ribbon cross-section (Fig. 9A) and the microstructure of the AZ91 alloy cast into metal mould (Fig. 9B), some significant differences are also easily noted in the morphological structure of alloy having the same chemical composition but cast by different methods and at different solidification rates.

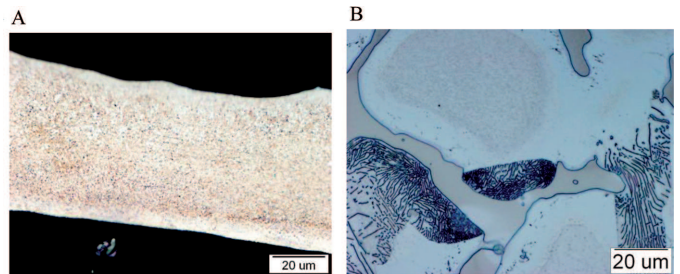


Fig. 9. A. Microstructure of AZ91 RS alloy ribbon cast by melt spinning; B. Microstructure of AZ91 alloy cast into metal mould

By measuring the overall dimensions of randomly selected cast ribbons, for the series of 1000 measurements, applying the methods of statistics, the values of the width (Table 3) and thickness (Figs. 10A, B, 11A, B, 12A, B) were determined.

TABLE 3

The width of a ribbon cast from AZ91RS alloy

| Unit               | [µm] |
|--------------------|------|
| Mean               | 1902 |
| Standard deviation | 275  |
| Maximum            | 2683 |
| Minimum            | 1385 |

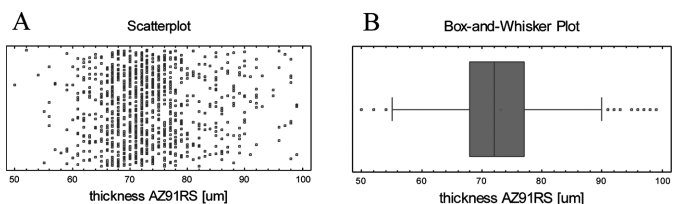


Fig. 10. A. A scatterplot of the thickness measurements taken on a ribbon cast from the AZ91RS alloy; B. A box-and-whisker plot with marked quartiles and a median for the thickness of a ribbon cast from the AZ91RS alloy



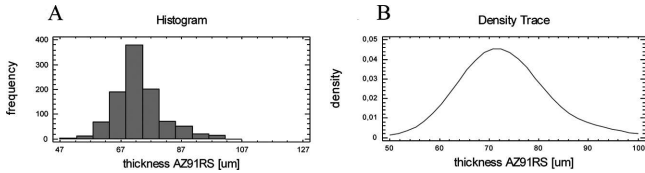


Fig. 11. A. Normal distribution of thickness values in a ribbon cast from the AZ91RS alloy; B. Normal distribution of thickness values in a ribbon cast from the AZ91RS alloy

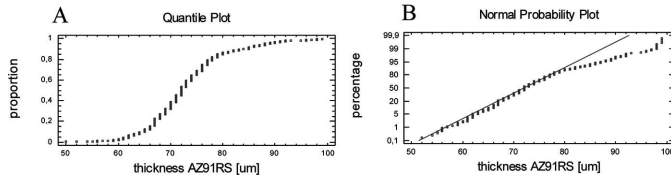


Fig. 12. A. Normal distribution of thickness values in a ribbon cast from the AZ91RS alloy; B. Normal distribution of thickness values in a ribbon cast from the AZ91RS alloy

**Third stage** of the process relates to the fragmentation of the cast RS strip.

The ribbon directly after casting is not suitable for consolidation, therefore it is first subjected to the process of fragmentation. This operation was performed in a high-speed mill for shear cutting. Additionally, the mill chamber was equipped with a 1 mm mesh classification screen, which allowed obtaining material with grains of a smaller size (Fig. 13A)

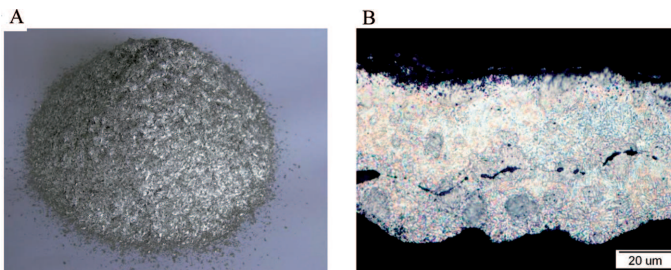


Fig. 13. A. Fragmented ribbons of AZ91RS alloy – the form of flakes; B. Microstructure on the cross-section of AZ91RS alloy ribbon – the form of flakes

The fragmented material was subjected to examinations under the microscope (Fig. 13B), showing the as-cast ribbon microstructure morphology.

To illustrate and define the characteristics of the fragmented strips, the bulk material was tested, and the results of measurements were helpful in further processes of cold compaction and hot consolidation. The granulometric analysis allowed determination of the grain size fractions and their respective quantities. Knowing the value of individual fractions it is possible to assess the effectiveness of the process of crushing.

It was stated that 95.2% of the granulate had particle size comprised in a range of (1.0-0.20) mm (Fig.14B). Tests were based on PN-EN 24497:1993 "Metal powders. Determination of the particle by dry sieving.

For chips of AZ91RS alloy, the bulk density and apparent density were determined (Fig. 14A). The calculated value of the bulk density of the ground chips was comprised in a range

of 385-405 g/l, and the apparent density ranged from 560 to 595 g/l.

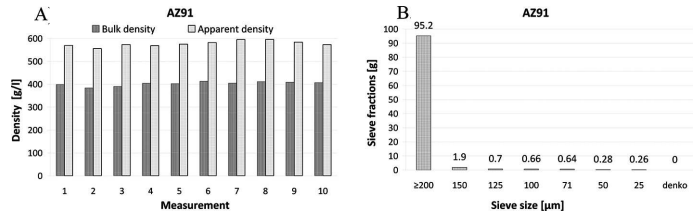


Fig. 14. A. Chart showing values of the bulk density and apparent density (for 10 measurements) of crushed chips made from the AZ91RS alloy; B. Graph showing fraction content of grains in the range of 1 mm - 200 µm - 0 µm / 100 g established in granulometric analysis of crushed chips from the AZ91RS alloy

The **fourth stage** of the process related to the compaction, consolidation and extrusion of crushed ribbons done on a vertical press of 60 T capacity to produce  $\phi$  8 rods (laboratory scale) and on a horizontal 500 T capacity press to produce  $\phi$  7 rods (semi-industrial scale).

On both presses, i.e. vertical of 60 T capacity and horizontal of 500 T capacity, the extrusion was carried out as a two-step process. The first step concerned the cold powder pre-compaction, the second step included consolidation and hot extrusion at 350°C -370°C yielding rods of  $\phi$  8 mm at  $\lambda = 14$  and the ram speed of 0.2 mm/s.

The parameters of the process of consolidation and extrusion on a horizontal 500 T press were as follows: 350°C ( $\pm 5^\circ\text{C}$ ) – the temperature of the ingot and 370°C ( $\pm 5^\circ\text{C}$ ) – the temperature of the recipient for rods of 5x  $\phi$  7 mm for  $\lambda = 41$  and the ram speed of 0.5 mm/s.

As a result of the hot direct extrusion of  $\phi$  8 mm rods on a 60 T press and  $\phi$  7 mm rods on a 500 T press, positive results of the work were achieved.

The following are examples of the microstructure of material produced in the process of consolidation and hot extrusion.

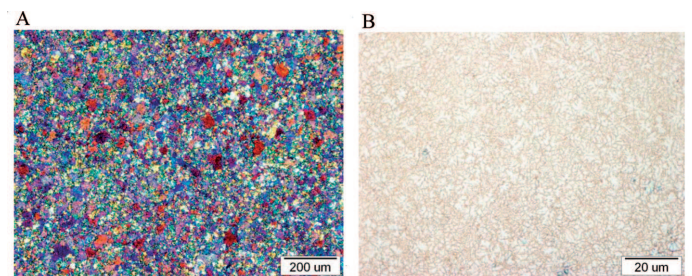


Fig. 15. A,B Microstructure of AZ91RS alloy consolidated by direct hot extrusion

Additionally, the mechanical properties of the material in unprocessed state (F) were determined. A comparison is given in Table 4.

TABLE 4

Mechanical properties of the AZ91 magnesium alloy cast by RS and extruded on a 500 T press (values given in the table refer to the state F)

| Properties   | Rm [MPa] | Rp0.2 [MPa] | A [%] | HBW | HV  |
|--------------|----------|-------------|-------|-----|-----|
| RS extrusion | 360      | 270         | 8     | 80  | 104 |

### 3. Summary and conclusions

The stages of the production technology to make extruded products with ultrafine grain structure from the cast AZ91 alloy, proposed and described in this article, enable obtaining final products.

The fragmented material is consolidated in the course of the final extrusion to form a solid profile with mechanical properties superior to the material of the same chemical composition but different structure cast into metal mould.

Examining images of the RS alloy microstructure, it is easy to note a different morphology of the precipitates of the alloying constituents as compared to the alloy cast into metal mould. The size of these constituents is also totally different.

The method of casting by melt spinning, combined with the process of plastic working, may enhance the technical value of alloys previously overlooked due to low properties and may result in an extension of the range of new alloys with new compositions.

The components made from the RS alloy may have smaller wall cross-sections, while maintaining an adequate level of the strength required. This relationship enables a weight reduction in machine parts for transport and translates into reduced fuel consumption and reduced level of harmful emissions.

This raises an important issue of the recycling of used products made from the RS materials. When the scrap of ultrafine grain structure is remelted in furnaces together with alloys obtained by conventional technology, there is no need to search for the methods of scrap classification, since its components create no threat of the permanent melt contamination.

#### REFERENCES

- [1] P.J. Meschter, J.E. O'neal, Rapid solidification processing of magnesium-lithium alloys, *Metallurgical Transactions A* **15**, 1, 237-240 (1984).
- [2] L.A. Dobrzański, *Materiały inżynierskie i projektowanie materiałowe*, WNT, Warszawa 2006, pp. 642-658.
- [3] Z. Górny, J. Sobczak, *Nowoczesne tworzywa odlewnicze na bazie metali nieżelaznych*, Kraków 2005.
- [4] P.J. Meschter, Microstructures and properties of rapidly solidified Mg-10Al and Mg-12.5Al-1.5Si alloys, *Metallurgical Transactions A* **18**, 2, 347-350, February 1987.
- [5] Instrukcja obsługi urządzenia UMSA, Kanada 2009.
- [6] J. Lelito, P.L. Zak, A.A. Shirzadi, A.L. Greer, W.K. Krajewski, J.S. Suchy, K. Haberl, P. Schumacher, Effect of SiC Reinforcement Particles on the Grain Density in a Magnesium Based Metal-Matrix Composite: Modelling and Experiment, *Acta Materialia* **60**, 2950-2958, April 2012.
- [7] J. Lelito, P.L. Zak, A.L. Greer, J.S. Suchy, W.K. Krajewski, B. Gracz, M. Szucki, A.A. Shirzadi, Crystallization Model of Magnesium Primary Phase in the AZ91/SiC Composite, *Composites: Part B* **43**, 3306-3309 (2012).
- [8] J. Lelito, P. Zak, J.Sz. Suchy, W. Krajewski, A.L. Greer, P. Darłak, Experimental Determination of Grain Density Function of AZ91/SiC Composite with Different Mass Fraction of SiC and Undercoolings Using Heterogeneous Model, *China Foundry* **8** (1), 101-106 (2011).
- [9] J.Sz. Suchy, J. Lelito, B. Gracz, P.L. Zak, H. Krawiec, Modelling of Composite Crystallization, *China Foundry* **9**, 2, 184-188 (2012).

*The study was financed from a Strategic „ZAMAT” Project No. POIG.01.03.01-00-015/09 entitled “Advanced materials and technologies for their production,” co-financed from the structural fund; the project implementation period is 2010-2013.*